Automatica 140 (2022) 110235

Contents lists available at ScienceDirect

Automatica

journal homepage: www.elsevier.com/locate/automatica

Robust formation control for networked robotic systems using Negative Imaginary dynamics☆

Junyan Hu [a,*], Barry Lennox [b], Farshad Arvin [b,*]

[a] Department of Computer Science, University College London, London, WC1E 6BT, UK
[b] Department of Electrical and Electronic Engineering, The University of Manchester, Manchester, M13 9PL, UK

ARTICLE INFO

Article history:
Received 12 November 2020
Received in revised form 10 June 2021
Accepted 27 January 2022
Available online 17 March 2022

Keywords:
Multi-robot systems
Swarm robotics
Negative Imaginary systems
Fault-tolerant control
Robustness

ABSTRACT

This paper proposes a consensus-based formation tracking scheme for multi-robot systems utilizing the Negative Imaginary (NI) theory. The proposed scheme applies to a class of networked robotic systems that can be modelled as a group of single integrator agents with stable uncertainties connected via an undirected graph. NI/SNI property of networked agents facilitates the design of a distributed Strictly Negative Imaginary (SNI) controller to achieve the desired formation tracking. A new theoretical proof of asymptotic convergence of the formation tracking trajectories is derived based on the integral controllability of a networked SNI systems. The proposed scheme is an alternative to the conventional Lyapunov-based formation tracking schemes. It offers robustness to NI/SNI-type model uncertainties and fault-tolerance to a sudden loss of robots due to hardware/communication fault. The feasibility and usefulness of the proposed formation tracking scheme were validated by lab-based real-time hardware experiments involving miniature mobile robots.

1. Introduction

Negative Imaginary (NI) systems theory was introduced in Lanzon and Petersen (2008) and has gradually come into the limelight due to its potential applications in vibration control of lightly-damped flexible structures (Lanzon & Petersen, 2008; Liu, Lam, Zhu, & Kwok, 2019), cantilever beams (Bhikkaji, Reza Moheimani, & Petersen, 2012), robotic manipulators (Mabrok, Kallapur, Petersen, & Lanzon, 2014), in nano-positioning applications (Das, Pota, & Petersen, 2014), control of multi-agent NI systems (Tran, Garratt, & Petersen, 2020; Tran, Mabrok, Garratt, & Petersen, 2021; Wang, Lanzon, & Petersen, 2015a; Wang, Lanzon, & Petersen, 2015b), in controlling dissipative systems (Bhowmick & Patra, 2017; Kurawa, Bhowmick, & Lanzon, 2021), etc. Simplistically, the term NI refers to a class of LTI systems having a *negative imaginary* frequency response. That is, the imaginary part of an NI (SNI) transfer function remains non-positive (negative) $\forall \omega \in (0, \infty)$. The NI framework offers a simple closed-loop stability criterion that depends only on the steady-state gains of the system. Hence, it becomes useful for designing controllers for practical systems even when the exact mathematical model is not available (Bhowmick & Patra, 2020). NI theory has recently been extended to discrete-time LTI systems (Ferrante, Lanzon, & Ntogramatzidis, 2017; Liu & Xiong, 2017).

Formation control of multi-robot systems has been an active area of research in the robotics and control communities over the past two decades. Some of the potential applications of formation control include cooperative exploration, object transportation (Alonso-Mora, Baker, & Rus, 2017; Hu, Bhowmick, & Lanzon, 2021), search and rescue (Hu, Bhowmick, Jang, Arvin, & Lanzon, 2021), etc. With the advent of modern algebraic graph theory, consensus-based cooperative control of multi-agent systems has witnessed immense progress. Ren and Atkins (2007) and Ren and Sorensen (2008) did the pioneering work to develop static formation control techniques for a group of first-order and second-order agents connected via a graph. Later, the concept of time-varying formation control for linear multi-agent systems was proposed in Dong and Hu (2016). However, in most consensus-based formation control schemes, the global information of the network (e.g., the Laplacian matrix) is required. This affects the flexibility of a cooperative control scheme to handle the inclusion or exclusion of the agents during an ongoing mission. To overcome this limitation, Hu, Bhowmick, and Lanzon (2020) proposed a distributed adaptive formation tracking protocol for a group of networked mobile robots with multiple leaders,

☆ This work was supported by the EU Horizon 2020 RoboRoyale project [grant number 964492], the Engineering and Physical Sciences Research Council, UK [grant numbers EP/R026084/1 and EP/P01366X/1], and the Royal Academy of Engineering, UK [grant number CiET1819]. The material in this paper was not presented at any conference. This paper was recommended for publication in revised form by Associate Editor James Lam under the direction of Editor Ian R. Petersen.

* Corresponding author.
E-mail addresses: junyan.hu@ucl.ac.uk (J. Hu), Barry.Lennox@manchester.ac.uk (B. Lennox), Farshad.Arvin@manchester.ac.uk (F. Arvin).

https://doi.org/10.1016/j.automatica.2022.110235
0005-1098/

where the network topology was not required to be known in advance. Subsequently, Hu, Turgut, Lennox, and Arvin (2022), Mehdifar, Bechlioulis, Hashemzadeh, and Baradarannia (2020) and Verginis, Nikou, and Dimarogonas (2019) laid significant contributions in developing robust formation control techniques to deal with the inevitable model uncertainties. However, practical validation of such control schemes through real-world robotic experiments still poses significant and nontrivial challenges.

The primary motivation of applying NI systems theory to develop a leader-following formation control scheme for networked multi-robot systems is that many robotic systems (e.g. two-wheeled mobile robots with nonholonomic constraints (Skeik, Hu, Arvin, & Lanzon, 2019)) can be transformed into single integrator dynamics via input–output feedback linearization (Slotine & Li, 1991). Interestingly, a network of single integrator agents, being a multi-input–multi-output (MIMO) NI system, can be conveniently stabilized by a distributed SNI system in a positive feedback loop. Pioneering research has been done in this direction in Wang et al. (2015a), Wang et al. (2015b). In Wang et al. (2015b), a robust output feedback consensus problem for a network of homogeneous NI systems was addressed. Thereafter Wang et al. (2015a) extended the results of Wang et al. (2015b) to deal with a network of heterogeneous NI systems. Subsequently, Skeik et al. (2019) developed a formation control scheme, being inspired by Wang et al. (2015b), for networked single integrator agents on a directed, strongly-connected and balanced graph. Later, Tran et al. (2020) extended the ideas of Wang et al. (2015a) to develop a particular formation control methodology for a group of heterogeneous autonomous vehicles to facilitate time-invariant switching in a cluttered environment.

The progress and challenges mentioned above motivate us to develop a simple, consensus-based, robust formation tracking scheme for multi-robot systems that can be modelled as (or transformed into) a network of single integrator agents. The proposed scheme exploits the inherent NI property of networked single integrator dynamics and guarantees the existence of a distributed SNI controller. This paper also introduces a new methodology to establish the asymptotic convergence of the formation tracking trajectories by utilizing the integral controllability property of the networked SNI systems. To do so, we first extend the conventional eigenvalue loci technique (Belletrutti & MacFarlane, 1971; MacFarlane & Belletrutti, 1973) to distributed SNI systems. The proposed scheme offers robustness to NI/SNI-type model uncertainties and fault-tolerance in the event of a sudden loss of agents. Lab-based experiments were conducted on a group of miniature two-wheeled mobile robots to demonstrate the feasibility of the scheme in practice.

Notation: $\mathbb{R}$ and $\mathbb{C}$ denote the sets of all real and complex numbers, respectively. $\mathbb{R}^{m\times n}$ and $\mathbb{C}^{m\times n}$ denote respectively the sets of all real and complex matrices of dimensions $(m \times n)$. $\Re(\cdot)$ and $\Im(\cdot)$ express the real and the imaginary parts, respectively. $A^\top$, A^* and $\bar{A}$ denote the transpose, complex conjugate transpose and complex conjugate of a matrix A. $\mathscr{RH}_\infty^{m\times n}$ denotes the set of all real, rational, proper and asymptotically stable transfer function matrices of dimension $(m \times n)$. For a transfer function matrix $M(s)$, $M(j\omega)^* = M(-j\omega)^\top$. The real-Hermitian and imaginary-Hermitian parts of $M(s)$ are given by $\frac{1}{2}[M(j\omega) + M(j\omega)^*]$ and $\frac{1}{2j}[M(j\omega) - M(j\omega)^*]$. (A, B, C, D) denotes a state-space realization of a real, rational, proper transfer function matrix $M(s) = D + C(sI - A)^{-1}B$. $A \otimes B$ indicates the Kronecker product of two matrices.

2. Essential preliminaries

In this section, some valuable technical preliminaries, definitions and lemmas are presented which underpin the proofs of the main results of the paper.

2.1. Definitions for negative imaginary systems theory

In this subsection, we recall the definitions of NI and SNI systems.

Definition 1 (*NI System Mabrok et al., 2014*)**.** Let $G(s)$ be the real, rational, proper transfer function matrix of a finite-dimensional and square system without any poles in $\Re[s] > 0$. Then, $G(s)$ is said to be NI if

- $j[G(j\omega) - G(j\omega)^*] \geq 0$ for all $\omega \in (0, \infty)$ except the values of ω where $j\omega$ is a pole of $G(s)$;
- If $s = j\omega_0$ with $\omega_0 \in (0, \infty)$ is a pole of $G(s)$, then it is at most a simple pole and the residue matrix $\lim_{s\to j\omega_0}(s - j\omega_0)jG(s)$ is Hermitian and positive semidefinite;
- If $s = 0$ is a pole of $G(s)$, then $\lim_{s\to 0} s^kG(s) = 0$ for all $k \geq 3$ and $\lim_{s\to 0} s^2G(s)$ is Hermitian and positive semidefinite.

Definition 2 (*SNI System Lanzon & Petersen, 2008*)**.** Let $G(s)$ be the real, rational, proper transfer function matrix of a finite-dimensional and square system. Then, $G(s)$ is said to be SNI if $G(s)$ has no poles in $\Re[s] \geq 0$ and $j[G(j\omega) - G(j\omega)^*] > 0$ for all $\omega \in (0, \infty)$.

2.2. Eigenvalue loci theory

Like the Nyquist plot, the eigenvalue loci $\gamma_i(s)$ for $i \in \{1, 2, \ldots, m\}$ of a transfer function matrix $P(s)$ is a conformal mapping of the function $\det[P(s)]$ in a complex plane, known as the eigenvalue loci plane, when s traverses along the s-plane D-contour in the clockwise direction as shown in Fig. 3(b). For complete details of the eigenvalue loci theory, the literature (Belletrutti & MacFarlane, 1971) and MacFarlane and Belletrutti (1973) may be referred.

Theorem 1 (*Belletrutti & MacFarlane, 1971; MacFarlane & Belletrutti, 1973*)**.** *The negative feedback interconnection of a plant $G(s)$ and a controller $C(s)$ is stable if, and only if, the net sum of critical point $(-1, j0)$ encirclements of all the eigenvalue loci $\gamma_i(j\omega)$ of the loop transfer function $G(s)C(s)$ for $i \in \{1, 2, \ldots, m\}$ is counter-clockwise and equal to the number of RHP zeros of the open-loop characteristic polynomial. For open-loop stable cases, none of $\gamma_i(j\omega)$ should encircle the critical point in the complex plane.*

2.3. Graph theory notations

Consider a weighted and directed graph $\mathscr{G} = (\mathscr{V}, \mathscr{E}, \mathscr{A})$ with a non-empty set of nodes $\mathscr{V} = \{1, 2, \ldots, M\}$, a set of edges $\mathscr{E} \subset \mathscr{V} \times \mathscr{V}$, and the associated adjacency matrix $\mathscr{A} = \left[a_{ij}\right] \in \mathbb{R}^{M\times M}$. An edge rooted at the ith node and ended at the jth node is denoted by (i, j), which means that the information can flow from node i to node j. a_{ij} is the weight of the edge (j, i) and $a_{ij} > 0$ if $(j, i) \in \mathscr{E}$. The jth node is called a neighbour of the ith node if $(j, i) \in \mathscr{E}$. The in-degree matrix is defined as $\mathscr{D} = \text{diag}\{d_i\} \in \mathbb{R}^{M\times M}$ where $d_i = \sum_{j=1}^{M} a_{ij}$. The Laplacian matrix $L \in \mathbb{R}^{M\times M}$ of $\mathscr{G}$ is defined as $L = \mathscr{D} - \mathscr{A}$.

Consider a multi-robot system containing M robots and one target. The target can be observed by a subset of robots in the network. If the ith robot observes the target, an edge $(0, i)$ is said to exist between them with a pinning gain $p_i > 0$.

3. Stability of an integrator feedback scheme involving networked NI/SNI systems

This section will first discuss under which conditions a network of SNI systems retains the same property. Subsequently,

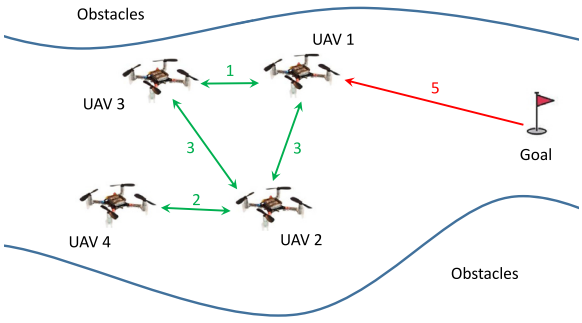

Fig. 1. An illustrative example of target tracking by networked UAVs.

the integral controllability property of networked SNI systems has been investigated in the homogeneous case. These results are essential prerequisites that will be invoked in Section 4 to develop a simple distributed formation control scheme for networked single integrator systems applying the NI toolkit.

3.1. Properties of networked SNI systems

We will now declare a technical assumption to be satisfied by the communication graphs corresponding to the network of SNI systems considered in this paper.

Assumption 1. The interaction among M agents is described by an undirected and connected graph $\mathcal{G}$. There always exists a root node which represents a leader (or a virtual target) and it provides the reference trajectory to the follower agents (at least to one follower).

According to Assumption 1, we have $L + P > 0$ where $P = \text{diag}\{p_1, p_2, \ldots, p_M\} > 0$ is the pinning-gain matrix. We will use the shorthand $\mathcal{L}_M = L + P$ throughout this paper. The following lemma proves that a network of homogeneous LTI systems exhibits SNI property if and only if an unit system is SNI.

Lemma 1. *Consider a group of M SNI agents $G(s) \in \mathcal{RH}_\infty^{m\times m}$ connected via a network topology $\mathcal{G}$ satisfying Assumption 1. Then, $\bar{G}(s) = \mathcal{L}_M \otimes G(s)$ is SNI if and only if $G(s)$ is SNI.*

Proof. (*Sufficiency*). Since $G(s)$ is SNI, it satisfies $j[G(j\omega) - G(j\omega)^*] > 0\ \forall\omega \in (0,\infty)$. Now we have $j[\bar{G}(j\omega) - \bar{G}(j\omega)^*] = j[\mathcal{L}_M \otimes G(j\omega) - \mathcal{L}_M^\top \otimes G(j\omega)^*] = \mathcal{L}_M \otimes j[G(j\omega) - G(j\omega)^*] > 0\ \forall\omega \in (0,\infty)$ [since $\mathcal{L}_M = \mathcal{L}_M^\top > 0$] by applying the Kronecker product property $A \otimes B > 0$ for $A = A^* > 0, B = B^* > 0$ (Horn & Johnson, 2012).

(*Necessity*). $j[\bar{G}(j\omega) - \bar{G}(j\omega)^*] > 0\ \ \forall\omega \in (0,\infty)$ implies $j[G(j\omega) - G(j\omega)^*] > 0\ \forall\omega \in (0,\infty)$ since $\mathcal{L}_M = \mathcal{L}_M^\top > 0$ due to Assumption 1. This completes the proof. ■

For better understanding of the network topology used in this paper, a practical example is shown in Fig. 1, where a team of unmanned aerial vehicles (UAVs) are navigated through a cluttered unknown environment via local information. Suppose that UAV 1 with advanced sensors can detect the position of the final destination (which can be viewed as a pinning node), thus an edge represented by the red single arrow is generated with a positive pinning gain. Other connected UAVs without goal detectors can only rely on neighbouring position information to reach the goal, the communication links among each other are represented by green double arrow with different positive edge weights.

3.2. Eigenvalue loci of networked SNI systems

So far in the literature, the eigenvalue loci theory (Belletrutti & MacFarlane, 1971; MacFarlane & Belletrutti, 1973) has been defined for a single LTI system. In this paper, being inspired by the developments of Bhowmick and Lanzon (2021) and Bhowmick and Patra (2018), the eigenvalue loci technique has been extended to homogeneous networked NI and SNI systems. The following lemma reveals that the eigenvalue loci of a homogeneous network of SNI systems stay within the third and fourth quadrants of a complex plane, termed as the eigenvalue loci plane, including (excluding) the real-axis in the open positive frequency interval, i.e., $\forall\omega \in (0,\infty)$.

Lemma 2. *Consider a group of M SNI agents $G(s) \in \mathcal{RH}_\infty^{m\times m}$ connected via a network topology $\mathcal{G}$ satisfying Assumption 1. Denote $\bar{G}(s) = \mathcal{L}_M \otimes G(s)$. Then, the eigenvalue loci $\gamma_i(j\omega)$ of $\bar{G}(s) \in \mathcal{RH}_\infty^{Mm\times Mm}$ lie strictly below the real-axis of the eigenvalue loci plane $\forall\omega \in (0,\infty)$ and $\forall i \in \{1, 2, \ldots, Mm\}$.*

Proof. We start this proof by recalling that $\bar{G}(s) = \mathcal{L}_M \otimes G(s)$ is SNI if and only if $G(s)$ is SNI via Lemma 1. Assume (λ_i, x_i) be an eigenvalue–eigenvector pair for $(\mathcal{L}_M \otimes G(j\omega)) \in \mathbb{C}^{Mm\times Mm}$ for $\omega \in (0,\infty)$ where $\lambda_i \in \mathbb{C}$ for $i \in \{1, 2, \ldots, Mm\}$ and $0 \neq x_i \in \mathbb{C}^{Mm}$. Note that in the case of repeated eigenvalues of $(\mathcal{L}_M \otimes G(j\omega))$ at an $\omega \in (0,\infty)$, only the linearly independent eigenvectors need to be considered. Now,

$$
\begin{aligned}
&x_i^*\,(\mathcal{L}_M \otimes G(j\omega))\,x_i \\
=&x_i^*\Big[\mathcal{L}_M \otimes [\frac{1}{2}(G(j\omega) + G^*(j\omega)) + j\frac{1}{2j}(G(j\omega) - G^*(j\omega))]\Big]x_i \\
=&x_i^*\,(\mathcal{L}_M \otimes A)\,x_i + j\,x_i^*\,(\mathcal{L}_M \otimes B)\,x_i \qquad (1)
\end{aligned}
$$

where $A = \frac{1}{2}[G(j\omega) + G^*(j\omega)]$ and $B = \frac{1}{2j}[G(j\omega) - G^*(j\omega)]$. Considering an orthonormal eigenvector $\|x_i\|_2 = 1$, without loss of generality, we obtain

$$x_i^*\,(\mathcal{L}_M \otimes G(j\omega))\,x_i = \lambda_i(x_i^* x_i) = \lambda_i\|x_i\|_2 = \Re[\lambda_i] + j\,\Im[\lambda_i]. \qquad (2)$$

Upon comparing (1) and (2), we have $\Re[\lambda_i] = x_i^*\,(\mathcal{L}_M \otimes A)\,x_i$ and $\Im[\lambda_i] = x_i^*\,(\mathcal{L}_M \otimes B)\,x_i$, both of which are real and scalar quantities since $A = A^*$, $B = B^*$ and $\mathcal{L}_M = \mathcal{L}_M^\top > 0$. Now, $B < 0\ \forall\omega \in (0,\infty)$ since $G(s)$ is SNI using Definitions 1 and 2. This then implies $\lambda_i[\mathcal{L}_M \otimes B] = \lambda_j[\mathcal{L}_M]\lambda_k[B] < 0\ \forall\omega \in (0,\infty)$ and $\forall i \in \{1, 2, \ldots, Mm\}$ via the distributive property of the eigenvalues of the Kronecker product of two matrices (Horn & Johnson, 2012). Therefore, for SNI systems, we have $\Im[\lambda_i\{\mathcal{L}_M \otimes G(j\omega)\}] < 0\ \forall\omega \in (0,\infty)$ and $\forall i$. This hence proves that all $\gamma_i(j\omega)$ of the network of homogeneous SNI systems lie strictly below the real-axis of the eigenvalue loci plane $\forall\omega \in (0,\infty)$. ■

Note that although the eigenvalue loci of the SNI systems $G(s) \in \mathcal{RH}_\infty^{m\times m}$ do not touch the real axis of the eigenvalue loci plane for any $\omega \in (0,\infty)$, each locus originates from (at $\omega = 0$) and terminate to (at $\omega = \infty$) the real axis since $G(0) = G(0)^\top$ and $G(\infty) = G(\infty)^\top$.

3.3. 'Integral controllability' of networked SNI systems

This subsection investigates the asymptotic stability of an integrator feedback control scheme (Fig. 2) containing networked SNI systems when the integral gain factor k is varied within a finite range. This property is referred to in this paper as *integral controllability* (IC) of networked SNI systems. This result (derived in Lemma 3) will be utilized later in Section 4 to develop a simple distributed formation control scheme for networked single integrator agents.

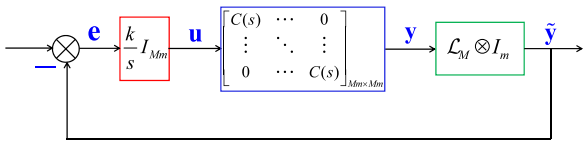

Fig. 2. An integrator feedback control scheme for networked SNI systems.

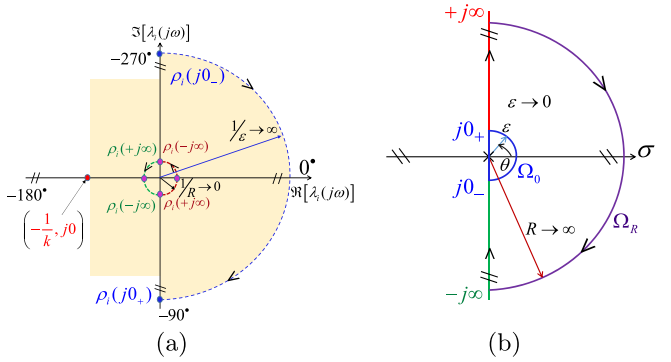

Fig. 3. (a) All the eigenvalue loci $\gamma_i(j\omega)$ of $\mathscr{L}_M \otimes \frac{1}{s}C(s)$ remain confined within the Yellow coloured region $\forall \omega \in \mathbb{R} \cup \{\infty\}$ when $C(s)$ is an SNI transfer function having $C(0) > 0$; and (b) Nyquist $\mathscr{D}$-contour in the s-plane. (For interpretation of the references to colour in this figure legend, the reader is referred to the web version of this article.)

Lemma 3. *Consider a group of M SNI systems $C(s) \in \mathscr{RH}_\infty^{m\times m}$ with $C(0) > 0$ connected via a network topology $\mathscr{G}$ that satisfies Assumption 1. Then, there exists a finite $k^\star > 0$ such that the negative feedback interconnection of $\mathscr{L}_M \otimes C(s)$ and $I_{Mm} \otimes \frac{k}{s}$, in Fig. 2, remains asymptotically stable for all $k \in (0, k^\star]$.*

Proof. In this proof, the notation $\gamma_i(s)$ is used to represent the eigenvalue loci of the loop transfer function matrix $\left(\mathscr{L}_M \otimes \frac{1}{s}C(s)\right)$. The negative feedback closed-loop networked interconnection of $[\mathscr{L}_M \otimes C(s)]$ and $\frac{k}{s}I_{Mm}$, remains asymptotically stable for any k in the range $(0, k^\star]$ if none of the eigenvalue loci $\gamma_i(j\omega)$ intersects the negative real-axis of the eigenvalue loci plane at any $\omega \in [-\infty, \infty]$. The above condition implies that none of the $\gamma_i(j\omega)$ will encircle the critical point $(-\frac{1}{k} + j0)$ for any $k \in (0, k^\star]$ using Theorem 1. Note that the upper limit $k^\star > 0$ depends on the maximum eigenvalue of the DC loop gain of $[\mathscr{L}_M \otimes C(s)]$ in Fig. 2. Let the Nyquist D-contour in the s-plane be indented at the origin to exclude the pole of the integrators. As shown in Fig. 3(b), we denote the points on (i) the semi-circle around the origin having infinitesimal radius by Ω_0, (ii) the rest of the $j\omega$-axis by $\Omega_{\pm j}$ and (iii) the RHP semi-circle having infinite radius by Ω_R; mathematically,

$$\Omega_0 = \{s |\ s = \varepsilon e^{j\theta},\ \varepsilon \in \mathbb{R}_{>0},\ \varepsilon \to 0_+,\ -\frac{\pi}{2} \le \theta \le \frac{\pi}{2}\},$$
$$\Omega_{\pm j} = \{s |\ s = j\omega,\ \omega \in (-\infty, 0) \cup (0, \infty)\},$$
$$\Omega_R = \{s |\ s = Re^{j\theta},\ R \in \mathbb{R}_{>0}, R \to +\infty,\ -\frac{\pi}{2} \le \theta \le \frac{\pi}{2}\}.$$

We will now establish via Parts I, II and III that all the eigenvalue loci $\gamma_i(s)$ stay within the Yellow coloured region in Fig. 3(a).

Part I: When $s \in \Omega_0$ Below, we show that the eigenvalue loci $\gamma_i(s)$ of $\left(\mathscr{L}_M \otimes \frac{1}{s}C(s)\right)$, where $C(s)$ is an SNI transfer function with $C(0) > 0$, lie within the Yellow semicircle having infinite radius (at the right-hand side of the imaginary axis), as shown Fig. 3(a), when the complex frequency variable s makes a complete traversal along the D-contour in the s-plane [see Fig. 3(b)], which is an union of the sets Ω_0, $\Omega_{\pm j}$ and Ω_R. The eigenvalue loci $\gamma_i(s)$ can be approximately expressed as

$$\gamma_i(s)|_{s\in\Omega_0} \simeq \lambda_i\left[\mathscr{L}_M \otimes C(0)\right]\frac{1}{\varepsilon}e^{-j\theta} \tag{4}$$

$\forall i \in \{1, 2, \ldots, Mm\}$, which can be further simplified as

$$\gamma_i(s)|_{s\in\Omega_0} \simeq \frac{m_i}{\varepsilon}e^{j(\phi_i-\theta)} \quad \forall i \in \{1, 2, \ldots, Mm\} \tag{5}$$

on setting $\lambda_i\left[\mathscr{L}_M \otimes C(0)\right] = m_i e^{j\phi_i}$ where $\phi_i = 0\ \forall i$ as $C(0) > 0$ and $\mathscr{L}_M > 0$. Therefore, $\gamma_i(j0_+) \simeq \frac{m_i}{\varepsilon}e^{-j\frac{\pi}{2}} \to +\infty\angle -\frac{\pi}{2}$ as $\varepsilon \to 0_+$ and when $\theta = \frac{\pi}{2}$ and similarly, $\gamma_i(j0_-) \to +\infty\angle +\frac{\pi}{2}$. This implies $-\frac{\pi}{2} \le \angle\gamma_i(j\omega) \le \frac{\pi}{2}$ when $s \in \Omega_0$. Hence, no infinite crossover occurs on the negative real-axis when each eigenvalue locus $\gamma_i(j\omega)$ encloses the zero-frequency points $\gamma_i(j0_-)$ and $\gamma_i(j0_+)$ via a semicircular arc of infinite radius in the clockwise direction, as illustrated in Fig. 3(a).

Part II: When $s \in \Omega_{\pm j}$ Let $\lambda_i\left[\mathscr{L}_M \otimes C(j\omega)\right] = m_i e^{j\phi_i}$ at each $\omega \in (0, \infty)$ and for all $i \in \{1, 2, \ldots, Mm\}$. Since $C(s)$ is SNI, $\phi_i(\omega) \in (-\pi, 0)\ \forall \omega \in (0, \infty)$ and hence, $\angle\gamma_i(j\omega) = (\phi_i - \frac{\pi}{2}) \in \left(-\frac{3\pi}{2}, -\frac{\pi}{2}\right)\ \forall \omega \in (0, \infty)$ and similarly, for all $\omega \in (-\infty, 0)$, $\angle\gamma_i(j\omega) \in \left(-\frac{3\pi}{2}, -\frac{\pi}{2}\right)$ as eigenvalue loci are symmetric with respect to real-axis. Therefore, when $s \in \Omega_{\pm j}$, all $\gamma_i(j\omega)$ stay within the Yellow rectangular region (at the left-hand side of the imaginary axis) marked shown in Fig. 3(a).

Part III: When $s \in \Omega_R$ For $s \in \Omega_R$, the eigenvalue loci $\gamma_i(s)$ where $i \in \{1, 2, \ldots, Mm\}$ can be expressed as

$$\gamma_i(s)|_{s\in\Omega_R} \simeq \lambda_i\left[\mathscr{L}_M \otimes C(\infty)\right]\frac{e^{-j\theta}}{R} = \frac{m_i}{R}e^{j(\phi_i-\theta)} \tag{6}$$

upon denoting $\lambda_i\left[\mathscr{L}_M \otimes C(\infty)\right] = m_i e^{j\phi_i}$. Now, $\gamma_i(+j\infty)$ can have three distinct positions depending on $C(\infty)$: (i) $\gamma_i(+j\infty) \to 0\angle -\frac{\pi}{2}$ when $C(\infty) > 0$; (ii) $\gamma_i(+j\infty) \to 0\angle -\pi$ when $C(\infty) = 0$; and (iii) $\gamma_i(+j\infty) \to 0\angle -\frac{3\pi}{2}$ when $C(\infty) < 0$. This then follows that each $\gamma_i(j\omega)$ encloses the infinite frequency points $\gamma_i(+j\infty)$ and $\gamma_i(-j\infty)$ through a semicircular arc of infinitesimal radius in the counter-clockwise direction [the Green and Red coloured dashed arcs drawn around the origin in Fig. 3(a)].

Parts I, II and III jointly prove that all $\gamma_i(s)$ stay within the Yellow coloured region shown in Fig. 3(a) and no infinite crossover occurs on the negative real-axis. This hence implies that there always exists a finite range of the integral gain factor $k \in (0, k^\star]$ such that the critical point $(-\frac{1}{k} + j0)$ is never encircled by any $\gamma_i(s)$. This guarantees the asymptotic stability of the negative feedback integrator-feedback scheme (in Fig. 2) via Theorem 1. ■

Remark 1. This paper extends the integral controllability (IC) property of NI and SNI systems, proposed in Bhowmick and Patra (2018) and Bhowmick and Lanzon (2021), to networked NI and SNI systems. Lemma 3 has exploited the IC property of a networked SNI system with positive definite DC-gain matrix, which is then invoked in Section 4 to develop a robust and fault-tolerant formation tracking scheme for feedback linearized robotic systems. An IC scheme facilitates asymptotic tracking and ensures closed-loop asymptotic stability for a finite range of the integral gain factor $k \in (0, k^\star]$ instead of the conventional PI controller that works only for particular values of $(k_p,\ k_i)$. The main advantage of the IC-based tracking scheme is that the closed-loop stability depends only on the positive definiteness of DC-gain matrix of the plant. Interestingly, all stable NI systems (including SNI as well) enjoy the symmetric DC-gain matrix property [as $C(0) = -CA^{-1}B + D = -CA^{-1}(-AYC^\top) + D = CYC^\top D = C(0)^\top$ via NI lemma (Lanzon & Petersen, 2008) and on noting that $D = D^\top$ is an assumption for all NI systems] and most of the practical SNI

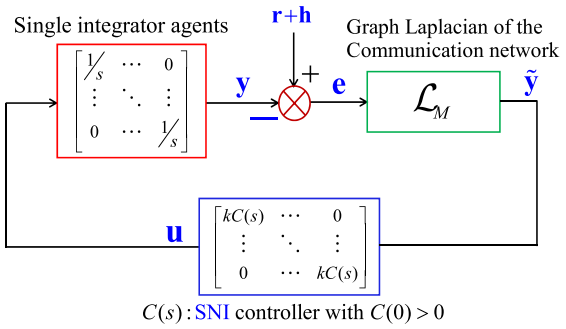

Fig. 4. A formation tracking scheme for a group of networked single integrator systems applying SNI theory.

systems have positive definite DC-gain. A networked SNI system preserves the positive definite DC-gain matrix property when the underlying graph Laplacian matrix satisfies the property $\mathscr{L}_M = L + P > 0$. Another advantage of using an IC-based tracking scheme is that it offers a convenient way of handling stable NI/SNI-type uncertainties depending only on their DC-gain (refer to Theorem 3).

4. A formation tracking control scheme for networked robotic systems using the SNI theory

This section presents this paper's main contribution, which develops a distributed formation control scheme for a class of multi-robot systems that can be modelled as (or transformed into) a group of networked single integrator agents with NI/SNI-type uncertainties. Note that many robotic systems can be feedback linearized into single integrator agents, e.g., two-wheeled mobile robots (please see Antonelli, Arrichiello, Caccavale, and Marino (2014), Ren and Sorensen (2008) and Tzafestas (2013) for more details). As a network of single integrator agents inherently satisfies the NI property with a pole at the origin, the formation tracking objectives can be effectively met by a distributed SNI controller depending only on the positive definiteness of the DC-gain matrix of the controller.

Before discussing the scheme, we declare the set of admissible reference input signals $\mathbf{r}(t)$ (generated by the leader node) to be followed by the agents.

Assumption 2. Let $\mathbf{r}(t) = \mathbf{1}_M r(t) \in \mathbb{R}^M \ \forall t \geq 0$ be the given tracking reference where $r(t)$ is continuous and bounded $\forall t \geq 0$ and $\lim_{t\to\infty} \mathbf{r}(t) = \mathbf{1}_M r_{ss} \triangleq \mathbf{r}_{ss}$ where $r_{ss} \not\equiv 0$ denotes the steady-state value of the reference signal $r(t)$ generated by the leader node.

Theorem 2, given next, will establish that, under the application of a MIMO, decoupled SNI controller $\text{diag}\{C(s), \ldots, C(s)\}$ where $C(s)$ is a single-input–single-output (SISO) SNI transfer function with $C(0) > 0$, a group of single integrator agents connected via a graph topology $\mathscr{G}$ satisfying Assumption 1 will asymptotically reach the desired formation and continue to track the leader.

Theorem 2. *Let M single integrator agents be connected via the topology $\mathscr{G}$, which satisfies Assumption 1. The set of admissible reference inputs $\mathbf{r}(t)$ satisfies Assumption 2 and let $\mathbf{h} = [h_1\ h_2\ \cdots\ h_M]^\top \in \mathbb{R}^M$ be the desired formation configuration vector. Let $C(s)$ be an SNI transfer function with $C(0) > 0$. Then, there exists a finite $k^\star > 0$ such that for any $k \in (0, k^\star]$, the single integrator agents (in Fig. 4) achieve formation tracking by the following distributed SNI output feedback control law*

$$u_i = kC(s)\sum_{j=1}^{M} a_{ij}\big((y_i - h_i) - (y_j - h_j)\big) + p_i(y_i - h_i - r) \tag{7}$$

where $i \in \{1, 2, \ldots, M\}$.

Proof. In this proof, the notations $\mathbf{E}(s)$, $\mathbf{Y}(s)$, $\mathbf{R}(s)$ will represent the Laplace transform of the real-valued, time-domain vector signals $\mathbf{e}(t) = [e_1(t)\ e_2(t)\ \cdots\ e_M(t)]^\top$, $\mathbf{y}(t) = [y_1(t)\ y_2(t)\ \cdots\ y_M(t)]^\top$ and $\mathbf{r}(t)\ \forall t \geq 0$. Note that the controller $C(s)$ is an SNI transfer function with $C(0) > 0$. With respect to Fig. 4, we define the formation trajectory tracking error as $\mathbf{e}(t) \triangleq \mathbf{r}(t) + \mathbf{h} - \mathbf{y}(t)$ and denote $\hat{\mathbf{r}} \triangleq \mathbf{r} + \mathbf{h}$. Now, we have

$$\mathbf{E}(s) = \left[I + (\mathscr{L}_M \otimes \frac{k}{s}C(s))\right]^{-1}\hat{\mathbf{R}}(s). \tag{8}$$

It is already established in Lemma 3 that the positive feedback consensus scheme shown in Fig. 4 is asymptotically stable under the application of the distributed SNI control law for all $k \in (0, \infty)$. The steady-state formation tracking error is found to be

$$\mathbf{e}_{ss} = \lim_{t\to\infty}\mathbf{e}(t) = \lim_{s\to 0} s\mathbf{E}(s) \tag{9a}$$

$$= \lim_{s\to 0} s\left[I_M + \left(\mathscr{L}_M \otimes \frac{k}{s}C(s)\right)\right]^{-1}\hat{\mathbf{R}}(s)$$

$$= \lim_{s\to 0} s\,[sI_M + (\mathscr{L}_M \otimes kC(s))]^{-1}\,(s\hat{\mathbf{R}}(s))$$

$$= [\mathscr{L}_M \otimes (kC(0))]^{-1}\left(\lim_{s\to 0} sI_M\right)\left(\lim_{s\to 0} s\left[\mathbf{R}(s) + \frac{1}{s}\mathbf{h}\right]\right)$$

$$= [0\ 0\ \cdots\ 0]^\top \tag{9b}$$

since $C(0) > 0$, $\mathscr{L}_M > 0$ and $\lim_{t\to\infty}\mathbf{r}(t) = \mathbf{1}_M r_{ss} = \mathbf{r}_{ss}$ via Assumption 2. The asymptotic convergence property of the trajectory tracking error, that is $\lim_{t\to\infty}\mathbf{e}(t) = \mathbf{0}$ implies $\mathbf{y}(t) \to \hat{\mathbf{r}}_{ss} = (\mathbf{r}_{ss} + \mathbf{h})$ as $t \to \infty$. ■

Remark 2. In Tran et al. (2020), the authors utilized the ideas of Wang et al. (2015a), Wang et al. (2015b) to develop a consensus scheme for a group of heterogeneous autonomous vehicles considering time-invariant topology switching. Although the results of Wang et al. (2015a), Wang et al. (2015b) and Tran et al. (2020) can be applied to solve the consensus problem for networked single integrator dynamics, the closed-loop state-space realization of the networked control system (i.e. the consensus scheme) used in Wang et al. (2015a), Wang et al. (2015b) and Tran et al. (2020) loses minimality due to a rank deficiency of the Laplacian matrix of an undirected graph, which may violate the internal stability of the scheme. On the contrary, the proposed consensus scheme in this paper does not face this problem as it considers a leader-following case for which $L + P > 0$.

Remark 3. In contrast to the Lyapunov stability approach used in most of the consensus-based formation control schemes, the proposed methodology relies on integral controllability theory and eigenvalue loci technique to prove asymptotic convergence of the formation trajectories. The proposed scheme also exhibits robustness to stable NI/SNI-type uncertainty when appears in input/output-multiplicative structure and $\mathscr{L}_2$-bounded external disturbances. Different from the conventional formation control strategies (e.g. Dong and Hu (2016), Hu, Bhowmick, Jang, et al. (2021) and Ren and Sorensen (2008)) that impose a particular distributed control law, the proposed NI-based scheme requires choosing only an SNI transfer function $C(s)$ with $C(0) > 0$. The asymptotic convergence is guaranteed for any SNI controller

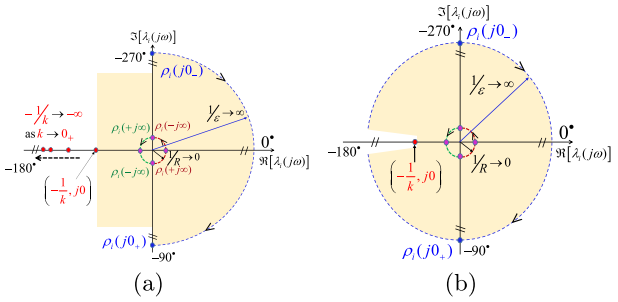

Fig. 5. (a) None of the eigenvalue loci $\gamma_i(j\omega)$ of $\mathscr{L}_M \otimes \frac{1}{s}C(s)$ does encircle the critical points $(-\frac{1}{k_i}, j0)$ for any $k_i \in [0, k^\star]$; and (b) All eigenvalue loci $\gamma_i(j\omega)$ of $\mathscr{L}_M \otimes C(s)[\frac{1}{s} + \delta(s)]$, where $\delta(s)$ is stable NI with $\delta(0) > 0$, $\delta(\infty) \geq 0$ and $C(s)$ is SNI with $C(0) > 0$, stay within the Yellow coloured region. (For interpretation of the references to colour in this figure legend, the reader is referred to the web version of this article.)

$C(s)$ with $C(0)$. Hence, in this paper, the proposed scheme offers greater flexibility to choose any structure of the controller to meet the desired performance specifications, which can be viewed a significant advantage over traditional consensus-based formation controllers.

4.1. Fault-tolerance to loss of robots

In the context of cooperative control of multi-robot systems, serious problems can be encountered following the sudden loss of agents, resulting from hardware faults or network failure. In such situations, it is essential to investigate how to preserve the stability of a network. Utilizing the ideas of Bhowmick and Patra (2018) and Bhowmick and Lanzon (2021), we will now establish that the proposed formation tracking scheme offers robust to a sudden loss of agents (i.e. robots). That is, upon occurrence of a fault, the control scheme maintains the overall stability of the network and also, a new stable operating condition is reached after an autonomous reconfiguration of the network, excluding the faulty agents. In the control scheme, the loss of an agent is modelled by making the gain of that particular channel equal to zero.

Lemma 4. *Under the suppositions of Theorem 2, the network of M single integrator agents in Fig. 4 achieves formation tracking by the distributed SNI output feedback control law (7) with k being replaced by $k_i \in [0, k^\star]$ $\forall i \in \{1, 2, \ldots, M\}$ where $k^\star > 0$ is finite.*

Proof. From Theorem 2, asymptotic stability of the formation tracking scheme for networked single integrator agents in Fig. 4 is guaranteed by the distributed SNI control law (7) for any $k_i \in (0, k^\star]$ and for each $i \in \{1, 2, \ldots, M\}$. This is equivalent to fulfilling the requirement that none of the eigenvalue loci $\gamma_i(s)$ of $\mathscr{L}_M \otimes \frac{1}{s}C(s)$ encircles the critical point $(-\frac{1}{k_i}, j0)$ for any value of $k_i \in (0, k^\star]$. When $k_i \to 0_+$ for some $i \in \{1, 2, \ldots, M\}$, the critical point $(-\frac{1}{k_i}, j0)$ approaches $(-\infty, j0)$ as depicted in Fig. 5(a). According to Theorem 2, all the eigenvalue loci $\gamma_i(j\omega)$ remain within the Yellow coloured region in Fig. 5(a) and therefore, no infinite crossover occurs on the negative real-axis. This hence ensures that none of the critical points $(-\frac{1}{k_i}, j0)$, where $k_i \in [0, k^\star]$, will be encircled by the eigenvalue loci $\gamma_i(j\omega)$. This implies that closed-loop stability remains preserved even when some of the channels are broken (indicated by $k_i = 0$). This completes the proof. ■

Remark 4. This paper has conceptualized the decentralized integral controllability (DIC) property of networked SNI systems taking the inspiration from (Bhowmick & Patra, 2018) that first

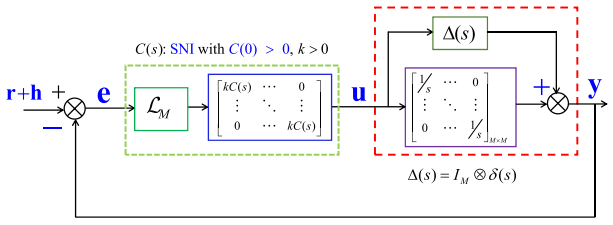

Fig. 6. An SNI-based formation tracking scheme for networked single integrator agents with a set of stable NI uncertainties $\delta(s)$ satisfying $\delta(0) > 0$ and $\delta(\infty) \geq 0$.

focussed on the DIC property of stable NI and SNI systems. DIC is an extended notion of IC, which gives the provision to vary the integral gains of each of the channels individually and allows even zero value of k, that is, DIC uses $k_i \in [0, k^\star]$ $\forall i \in \{1, 2, \ldots, M\}$ instead of $k \in (0, k^\star]$ used in case of IC. In the case of a sudden loss of agents due to hardware/communication failure, it is of utmost importance to maintain the stability of the overall network without readjusting the other parts. A loss of agent (for instance the ith agent) can be theoretically modelled by putting $k_i = 0$. The DIC property of a network ensures that the overall closed-loop stability remains preserved in the event of losing some of the agents [$k_i = 0$ for those i] without changing the controller or adjusting any part of the network.

4.2. Robustness to model uncertainty

This subsection examines the robustness of the NI-based formation tracking scheme against model uncertainties of the agents caused by either imprecise modelling or inexact feedback linearization. This study is particularly useful for the multi-robot systems that can be feedback linearized into single integrator dynamics along with an uncertainty appearing in additive/multiplicative form.

Theorem 3. *Let G_Δ be an uncertain LTI system that can be modelled as $G_\Delta(s) = \frac{1}{s} + \delta(s)$ where $\delta(s)$ is stable NI with $\delta(0) > 0$ and $\delta(\infty) \geq 0$. Consider a network of M such G_Δ agents connected via the topology $\mathscr{G}$, that satisfies Assumption 1. The set of admissible reference inputs $\mathbf{r}(t)$ satisfies Assumption 2 and let $\mathbf{h} = [h_1\ h_2\ \cdots\ h_M]^\top \in \mathbb{R}^M$ be the desired formation configuration vector. Then, there exists an SNI transfer function $C(s)$ with $C(0) > 0$ and a finite $k^\star > 0$ such that for any $k \in (0, k^\star]$, the agents achieve formation tracking in the presence of $\delta(s)$ by the distributed SNI output feedback control law (7).*

Proof. The negative feedback closed-loop networked system shown in Fig. 6 remains asymptotically stable in presence of any stable NI uncertainty $\delta(s)$ with $\delta(0) > 0$ and $\delta(\infty) \geq 0$ if none of the eigenvalue loci $\gamma_i(j\omega)$ of $\mathscr{L}_M \otimes C(s)[\frac{1}{s} + \delta(s)]$ encircles the critical point $(-\frac{1}{k}, j0)$ for any $k \in (0, k^\star]$. The proof proceeds along the similar track of Theorem 2. We will first show that all $\gamma_i(s)$ lie within the Yellow coloured region, illustrated in Fig. 5(b), in the presence of any $\delta(s)$, as described above.

When $s \in \Omega_0$, following the techniques adopted in Lemma 3, $\gamma_i(s)$ can be expressed as

$$\gamma_i(s)|_{s\in\Omega_0} = \lambda_i\left[\mathscr{L}_M \otimes C(0)\left(\frac{1}{\varepsilon}e^{-j\theta} + \delta(0)\right)\right] \tag{10}$$

$\forall i \in \{1, \ldots, M\}$, which can be closely approximated as

$$\gamma_i(s)|_{s\in\Omega_0} \simeq \lambda_i\left[\mathscr{L}_M \otimes C(0)\frac{1}{\varepsilon}e^{-j\theta}\right], \tag{11}$$

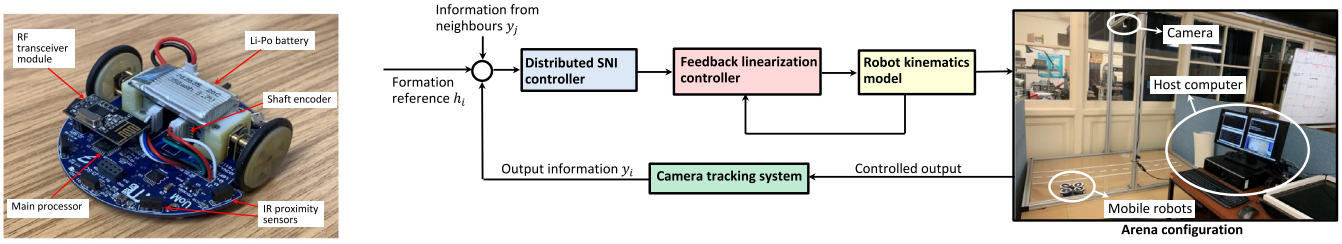

Fig. 7. (a) Mona robot (Arvin, Espinosa, Bird, West, Watson, & Lennox, 2019) used in the experimental validation; and (b) The hardware control loop implemented in our experiment. The experimental set-up also includes a camera tracking system and a host computer.

where $\mathscr{L}_M > 0$, $\delta(0) > 0$, $\varepsilon \to 0_+$ and $\theta \in [-\frac{\pi}{2}, \frac{\pi}{2}]$. Therefore, the infinite frequency points are computed as $\gamma_i(j0_+) \to \infty\angle -\frac{\pi}{2}$ when $\theta = \frac{\pi}{2}$, and similarly, $\gamma_i(j0_-) \to \infty\angle\frac{\pi}{2}$ with $\theta = -\frac{\pi}{2}$. Therefore, no infinite crossover takes place on the negative real-axis when the eigenvalue loci $\gamma_i(j\omega)$ enclose the zero-frequency points $\gamma_i(j0_-)$ and $\gamma_i(j0_+)$ through a semicircular arc of infinite radius in the clockwise direction, as illustrated in Fig. 5(b).

When $s \in \Omega_{\pm j}$, all the eigenvalue loci $\gamma_i(s)$ reside within the Yellow coloured region shown in Fig. 5(b) since $\angle\gamma_i(j\omega) = \angle\left[C(j\omega)(\frac{1}{j\omega} + \delta(j\omega))\right] \in (-2\pi, 0)\ \forall\omega \in (0, \infty)$ on noting that $\angle C(j\omega) \in (-\pi, 0)\ \forall\omega \in (0, \infty)$ as $C(s)$ is SNI and $\angle\delta(\omega) \in [-\pi, 0]\ \forall\omega \in (0, \infty)$ since $\delta(s)$ is stable NI. It is important to note here that although, during this interval, $\gamma_i(j\omega)$ intersect both the negative and positive real axes one/many times at finite distances from the origin, no infinite crossover takes place.

When $s \in \Omega_R$, each $\gamma_i(s)$ connects the infinite-frequency points $\gamma_i(+j\infty)$ and $\gamma_i(-j\infty)$ [see Fig. 5(b)], as explained in the proof of Theorem 2. This ensures that there always exists a finite upper bound of the integral gain $k^\star > 0$ such that for any $k \in (0, k^\star]$, the critical point $(-\frac{1}{k} + j0)$ remains unencircled by all $\gamma_i(s)$. Hence, closed-loop stability of the formation tracking remains preserved in the presence of any additive, stable NI uncertainty $\delta(s)$ with $\delta(0) > 0$ and $\delta(\infty) \geq 0$.

Then, following Theorem 2, the formation tracking error is given by $\mathbf{E}(s) = \left[I + (\mathscr{L}_M \otimes kC(s)(\frac{1}{s} + \delta(s)))\right]^{-1}\hat{\mathbf{R}}(s)$ where $\mathbf{e}(t) = \mathbf{r}(t) + \mathbf{h} - \mathbf{y}(t)\ \forall t \geq 0$ and denoting $\hat{\mathbf{r}} = \mathbf{r} + \mathbf{h}$. Finally, the steady-state formation tracking error is given by

$$\begin{aligned}\mathbf{e}_{ss} &= \lim_{t\to\infty}\mathbf{e}(t) = \lim_{s\to 0} s\mathbf{E}(s)\\ &= \lim_{s\to 0} s\left[I_M + \left(\mathscr{L}_M \otimes kC(s)(\frac{1}{s} + \delta(s))\right)\right]^{-1}\hat{\mathbf{R}}(s)\\ &= [0\ 0\ \cdots\ 0]^\top,\end{aligned}$$

since $C(0) > 0$, $\delta(0) > 0$, $\mathbf{h}$ is constant and $\lim_{t\to\infty}\mathbf{r}(t) = \mathbf{1}_M r_{ss}$ via Assumption 2. This hence confirms that the group of networked single integrator agents $G_\Delta(s) = \frac{1}{s} + \delta(s)$ achieve asymptotic formation tracking in presence of any additive-type $\delta(s)$ described above. ■

5. Experimental validation

To examine the feasibility and effectiveness of the proposed NI-based formation control scheme, small-scale hardware experiments involving miniature, two-wheeled mobile robots [Mona (Arvin et al., 2019) shown in Fig. 7(a)] were conducted. The hardware control loop is shown in Fig. 7(b) along with the experimental set-up, which utilizes a camera tracking system and a host computer. The position tracking system used in this experiment is an open-source multi-robotic localization system developed in Krajník, et al. (2014). The camera tracking system can track the positions and orientations of the robots by identifying the unique circular tags attached on top of the robots. The position information is transmitted to the controller via the ROS communication framework. An input–output feedback linearization technique was applied to transform the nonlinear kinematics of each two-wheeled mobile robot (Mona) into a decoupled two-input–two-output single integrator system ($\frac{1}{s}I_2$) following (Hu, Bhowmick, Jang, et al., 2021). Each robot had a safe zone of 0.1 m radius and was repelled from other robots entering within its safe zone. For simplicity, all the weight gains of the communication links are specified to be equal to 1. The control objectives considered in the experiment were to (i) first achieve a triangular formation by six mobile robots with respect to a given virtual target, (ii) then to keep tracking a planar moving target (in a straight line) without disrupting the formation, and (iii) to test the robustness of the proposed scheme against sudden loss of robots due to hardware/communication issues. The first experiment (Experiment 1) was done to validate the first two objectives, while the second one (Experiment 2) was conducted to validate the third objective. The video of the experiments can be found at https://www.youtube.com/watch?v=5V49vgJ3An0.

5.1. Experiment 1

This experiment was carried out using a group of six networked Mona robots to test the formation trajectory tracking under the application of a distributed SNI controller $C(s) = \frac{s^2+s+1}{(s+1)(2s+1)(s^2+2s+5)}I_2$ with $C(0) > 0$. Fig. 8(a) shows the initial positions of the robots and the virtual target (marked by •) on the arena. The communication graph is represented by green lines. Fig. 8(b) suggests that a triangular formation has been attained by those six robots surrounding the virtual target. As the virtual target moves from the left to the right side of the arena, the entire formation assembly keeps tracking it. Fig. 8(c) depicts that the triangular formation containing all six robots has reached the middle of the arena. Fig. 8(d) shows that the robots' formation finally reaches the right end of the arena and keeps tracking the virtual target. Fig. 9 plots the velocities of the left and right wheel motors acquired by the robots during the formation tracking. Fig. 10(a) and Fig. 10(b) portray the X-axis and Y-axis components of the formation tracking error $\varepsilon_i = y_i - h_i - r\ \forall i \in \{1, 2, \ldots, 6\}$ during the experiment. It can be noticed that the tracking error ε_i decays almost to zero after 25s, which implies that all six robots have achieved the desired formation surrounding the virtual target.

5.2. Experiment 2

This experiment was performed with four Mona robots to test the robustness of the proposed formation tracking scheme to a sudden loss of agents. The experiment started with the objective of achieving a square formation by the robots with respect to the given virtual target (marked by •). Fig. 11(a) shows the initial

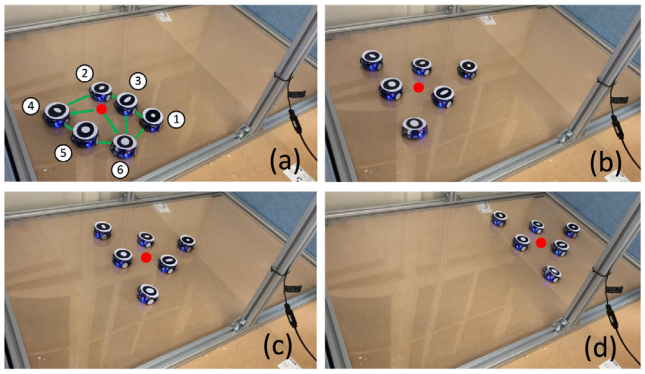

Fig. 8. Progress of the formation tracking mission being achieved by a team of six mobile robots during Experiment 1.

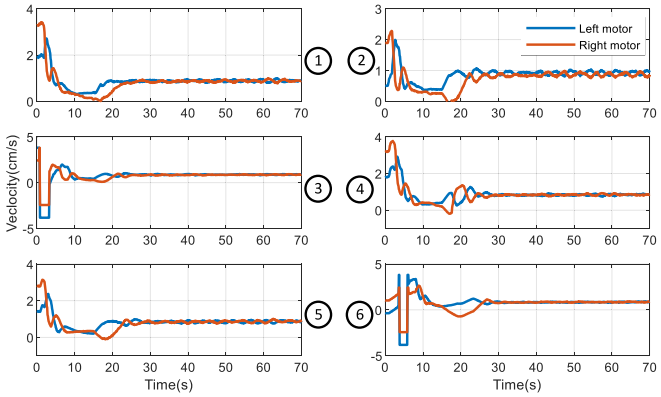

Fig. 9. Time-variation of the velocities of the left and right wheel motors acquired by the robots during the process of achieving the desired formation.

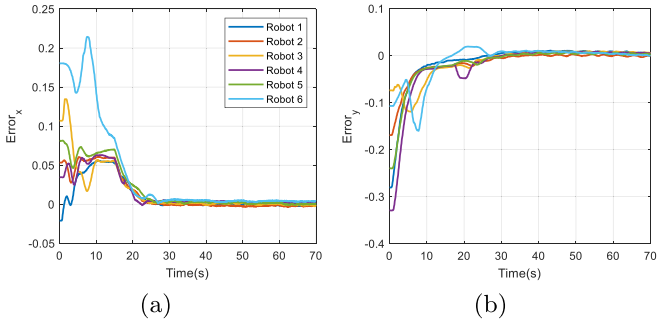

Fig. 10. Time evolvement of the formation trajectory tracking error $\varepsilon_i(t) = r_i + h_i - y_i(t)$ of all six robots during the experiment. (a) Error_x represents the component of ε_i along X-axis; (b) Error_y represents the component along Y-axis.

configuration of the robots on the arena, while Fig. 11(b) suggests that the desired square formation was attained by those four robots surrounding the virtual target. Fig. 11(c) shows that the entire formation kept on moving towards the centre of the arena following the moving virtual target. Fig. 11(c) gave rise to a situation when one of the robots (marked by X) stopped functioning due to a sudden fault. Fig. 11(d) shows that despite a sudden loss of one robot, the remaining three were able to tackle the situation and attained a new triangular formation with respect to the given target. Please note here that the switching from square formation to triangular formation was made possible via an autonomous network reconfiguration (implemented via a Matlab program) of the existing robots when one of them stopped operating due to a fault. During the transient phase, upon the occurrence of a fault,

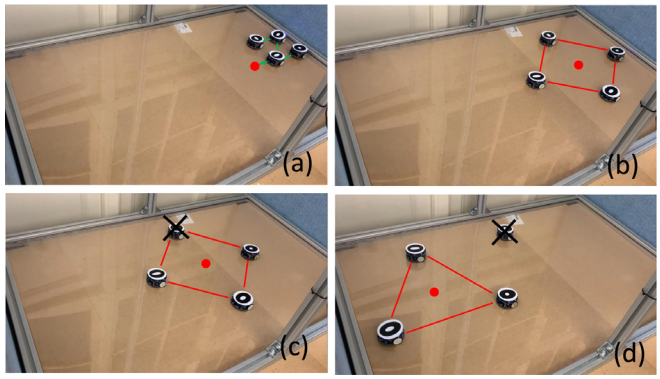

Fig. 11. Experiment 2 shows that a square formation is first attained by four Mona Robots, which is then switched to a triangular formation after a sudden loss of one robot.

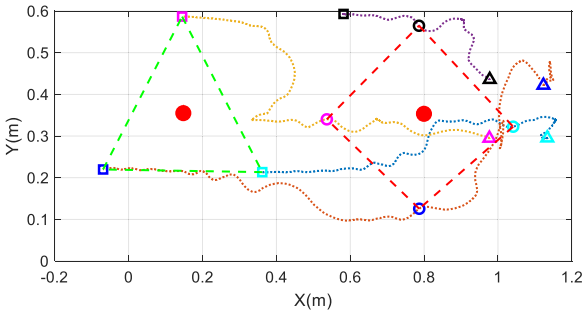

Fig. 12. Position trajectories of the robots during the formation tracking mission in Experiment 2.

the overall stability of the network is guaranteed via Lemma 4. Fig. 12 complements the results depicted in Figs. 11(a)– 11(d) by showing the spatial variation of the position trajectories of the robots during the experiment.

6. Conclusion

This paper has developed a consensus-based formation tracking scheme for a class of networked robotic systems that can be modelled as (or feedback linearized into) a team of single integrator agents. Owing to the NI property of networked single integrator agents connected via an undirected graph, a distributed SNI controller facilitates a formation tracking scheme with asymptotic convergence. The eigenvalue loci technique is used as an alternative to the conventional Lyapunov-based approaches to derive a theoretical proof of the proposed scheme. Lab-based experiments involving small-scale two-wheeled mobile robots were performed to show the feasibility of the scheme. In the future, the proposed scheme may be extended to handle the formation tracking problem for networked positive systems taking the ideas from Liu, Lam, and Shu (2020) and Yang, Yin, and Liu (2019).

Acknowledgement

The authors would like to gratefully acknowledge Dr Parijat Bhowmick, Indian Institute of Technology Guwahati, for his support and encouragement in preparing this paper.

References

Alonso-Mora, J., Baker, S., & Rus, D. (2017). Multi-robot formation control and object transport in dynamic environments via constrained optimization. *International Journal of Robotics Research*, *36*(9), 1000–1021.

Antonelli, G., Arrichiello, F., Caccavale, F., & Marino, A. (2014). Decentralized time-varying formation control for multi-robot systems. *International Journal of Robotics Research*, *33*(7), 1029–1043.
Arvin, F., Espinosa, J., Bird, B., West, A., Watson, S., & Lennox, B. (2019). Mona: an affordable open-source mobile robot for education and research. *Journal of Intelligent and Robotic Systems*, *94*(3), 761–775.
Belletrutti, J. J., & MacFarlane, A. G. J. (1971). Characteristic loci techniques in multivariable-control-system design. *Proceedings of the Institution of Electrical Engineers*, *118*(9), 1291–1297.
Bhikkaji, B., Reza Moheimani, S. O., & Petersen, I. R. (2012). A negative imaginary approach to modeling and control of a collocated structure. *IEEE/ASME Transactions on Mechatronics*, *17*(4), 717–727.
Bhowmick, P., & Lanzon, A. (2021). Applying negative imaginary systems theory to non-square systems with polytopic uncertainty. *Automatica*, *128*, 109570(1–14).
Bhowmick, P., & Patra, S. (2017). On LTI output strictly negative-imaginary systems. *Systems & Control Letters*, *100*, 32–42.
Bhowmick, P., & Patra, S. (2018). On decentralized integral controllability of stable negative-imaginary systems and some related extensions. *Automatica*, *94*, 443–451.
Bhowmick, P., & Patra, S. (2020). Solution to negative-imaginary control problem for uncertain LTI systems with multi-objective performance. *Automatica*, *112*, 1–9.
Das, S. K., Pota, H. R., & Petersen, I. R. (2014). Resonant controller design for a piezoelectric tube scanner: A 'mixed' negative-imaginary and small-gain approach. *IEEE Transactions on Control Systems Technology*, *22*(5), 1899–1906.
Dong, X., & Hu, G. (2016). Time-varying formation control for general linear multi-agent systems with switching directed topologies. *Automatica*, *73*, 47–55.
Ferrante, A., Lanzon, A., & Ntogramatzidis, L. (2017). Discrete-time negative imaginary systems. *Automatica*, *79*, 1–10.
Horn, R. A., & Johnson, C. R. (2012). *Matrix analysis* (second ed.). New York, USA: Cambridge University Press.
Hu, J., Bhowmick, P., Jang, I., Arvin, F., & Lanzon, A. (2021). A decentralized cluster formation containment framework for multirobot systems. *IEEE Transactions on Robotics*, *37*(6), 1936–1955.
Hu, J., Bhowmick, P., & Lanzon, A. (2020). Distributed adaptive time-varying group formation tracking for multi-agent systems with multiple leaders on directed graphs. *IEEE Transactions on Control of Network Systems*, *7*(1), 140–150.
Hu, J., Bhowmick, P., & Lanzon, A. (2021). Group coordinated control of networked mobile robots with applications to object transportation. *IEEE Transactions on Vehicular Technology*, *70*(8), 8269–8274.
Hu, J., Turgut, A. E., Lennox, B., & Arvin, F. (2022). Robust formation coordination of robot swarms with nonlinear dynamics and unknown disturbances: Design and experiments. *IEEE Transactions on Circuits and Systems II: Express Briefs*, *69*(1), 114–118.
Krajník, T., Nitsche, M., Faigl, J., Vaněk, P., Saska, M., Přeučil, L., et al. (2014). A practical multirobot localization system. *Journal of Intelligent and Robotic Systems*, *76*(3–4), 539–562.
Kurawa, S., Bhowmick, P., & Lanzon, A. (2021). Negative imaginary theory for a class of linear time-varying systems. *IEEE Control Systems Letters*, *5*(3), 1001–1006.
Lanzon, A., & Petersen, I. R. (2008). Stability robustness of a feedback interconnection of systems with negative imaginary frequency response. *IEEE Transactions on Automatic Control*, *53*(4), 1042–1046.
Liu, J. J. R., Lam, J., & Shu, Z. (2020). Positivity-preserving consensus of homogeneous multiagent systems. *IEEE Transactions on Automatic Control*, *65*(6), 2724–2729.
Liu, M., Lam, J., Zhu, B., & Kwok, K.-W. (2019). On positive realness, negative imaginariness, and $\mathscr{H}_\infty$ control of state-space symmetric systems. *Automatica*, *101*, 190–196.
Liu, M., & Xiong, J. (2017). Properties and stability analysis of discrete-time negative imaginary systems. *Automatica*, *83*, 58–64.
Mabrok, M. A., Kallapur, A. G., Petersen, I. R., & Lanzon, A. (2014). Generalizing negative imaginary systems theory to include free body dynamics: Control of highly resonant structures with free body motion. *IEEE Transactions on Automatic Control*, *59*(10), 2692–2707.
MacFarlane, A. G. J., & Belletrutti, J. J. (1973). The characteristic locus design method. *Automatica*, *9*(5), 575–588.
Mehdifar, F., Bechlioulis, C. P., Hashemzadeh, F., & Baradarannia, M. (2020). Prescribed performance distance-based formation control of multi-agent systems. *Automatica*, *119*, Article 109086.
Ren, W., & Atkins, E. (2007). Distributed multi-vehicle coordinated control via local information exchange. *International Journal of Robust and Nonlinear Control*, *17*(10–11), 1002–1033.
Ren, W., & Sorensen, N. (2008). Distributed coordination architecture for multi-robot formation control. *Robotics and Autonomous Systems*, *56*(4), 324–333.
Skeik, O., Hu, J., Arvin, F., & Lanzon, A. (2019). Cooperative control of integrator negative imaginary systems with application to rendezvous multiple mobile robots. In *Proceedings of 12th IEEE international workshop on robot motion and control* (pp. 15–20).
Slotine, J.-J. E., & Li, W. (1991). *Applied nonlinear control*. Englewood Cliffs, NJ: Prentice-Hall.
Tran, V. P., Garratt, M., & Petersen, I. R. (2020). Switching time-invariant formation control of a collaborative multi-agent system using negative imaginary systems theory. *Control Engineering Practice*, *95*, Article 104245.
Tran, V. P., Mabrok, M. A., Garratt, M. A., & Petersen, I. R. (2021). Hybrid adaptive negative imaginary- neural-fuzzy control with model identification for a quadrotor. *IFAC Journal of Systems and Control*, *16*, 100156(1–13).
Tzafestas, S. G. (2013). *Introduction to mobile robot control*. Elsevier.
Verginis, C. K., Nikou, A., & Dimarogonas, D. V. (2019). Robust formation control in $\mathbb{SE}(3)$ for tree-graph structures with prescribed transient and steady state performance. *Automatica*, *103*, 538–548.
Wang, J., Lanzon, A., & Petersen, I. R. (2015a). Robust cooperative control of multiple heterogeneous negative-imaginary systems. *Automatica*, *61*, 64–72.
Wang, J., Lanzon, A., & Petersen, I. R. (2015b). Robust output feedback consensus for networked negative-imaginary systems. *IEEE Transactions on Automatic Control*, *60*(9), 2547–2552.
Yang, N., Yin, Y., & Liu, J. (2019). Positive consensus of directed multi-agent systems using dynamic output-feedback control. In *Proceedings of 58th IEEE conference on decision and control* (pp. 897–902).

Junyan Hu received B.Eng. degree in Automation from Hefei University of Technology in 2015 and Ph.D. degree in Electrical and Electronic Engineering from the University of Manchester in 2020.

Dr. Hu is currently a Lecturer in Robotics with University College London (UCL). From 2019 to 2021, he worked as a Research Associate with the University of Manchester. His research interests include swarm robotics, intelligent control, sensor networks, and autonomous systems. He has been serving as a reviewer for many top/leading journals and conferences in the field of robotics and artificial intelligence.

Barry Lennox is a Professor of Applied Control and Nuclear Engineering Decommissioning and holds a Royal Academy of Engineering Chair in Emerging Technologies. He is Director of the Robotics and Artificial Intelligence for Nuclear (RAIN) Robotics Hub and Research Director of the Dalton Cumbrian Facility. He is a Fellow of the Royal Academy of Engineering, Senior Member of the IEEE, Fellow of the IET and InstMC, and a Chartered Engineer. He is an expert in applied control and its use in robotics and process operations and has considerable experience in transferring leading edge technology into industry.

Farshad Arvin is an Associate Professor in Robotics at the Department of Electrical & Electronic Engineering in the University of Manchester. He received his B.Sc. degree in Computer Hardware Engineering in 2004, M.Sc. degree in Computer Systems Engineering in 2010, and a Ph.D. in Computer Science in 2015. His research interests include swarm robotics and autonomous systems. Farshad joined the University of Manchester in July 2015 as a Post-Doctoral Researcher at the Department of Electrical and Electronic Engineering. He was a Research Assistant at the Computational Intelligence Laboratory (CIL) in the University of Lincoln, UK (2012 to 2015). He was awarded a Marie Curie-Sklodowska Fellowship to be involved in the FP7-EYE2E and LIVCODE EU projects during his Ph.D. study. He visited several leading institutes including Artificial Life Laboratory in University of Graz, Austria in 2018, the Italian Institute of Technology (iit) in Genoa, Italy in 2017, Institute of Rehabilitation and Medical Robotics in Huazhong University of Science and Technology (HUST), Wuhan, China in 2014, and the Institute of Microelectronics at Tsinghua University in Beijing, in 2012 and 2013.

Farshad is the founding director of Swarm & Computation Intelligence Laboratory (SwaCIL) formed in 2018. He is coordinating several research projects including a large EU project H2020-FET RoboRoyale and he is a PI in H2020-FET Robocoenosis.